Supporting information

Purine-Based Ir(III) Complexes for Sensing Viscosity of Endoplasmic Reticulum with Fluorescence Lifetime Imaging Microscopy

Xin Liu, Kun Li,* Lei Shi, Hong Zhang, Yan-Hong Liu, Hao-Yuan Wang, Nan Wang, Xiao-Qi Yu*

*Key Laboratory of Green Chemistry and Technology, Ministry of Education, College of Chemistry, Sichuan University, No. 29, Wangjiang Road, Chengdu, 610064, P.R. China. *Correspondence and requests for materials should be addressed to Kun Li (kli@scu.edu.cn) or Xiao-Qi Yu (xqyu@scu.edu.cn)*

Contents

1. Experimental Sections

1.1 General information

All chemicals and solvents were commercially available and were used without further purification. 2,6-dichloropurine, methyl iodide, potassium carbonate, tetra-(triphenylphosphine) palladium, and ammonium hexafluorophosphate, Iridium chloride, phenylboronic acid, 2-methylphenylboronic acid were purchased from aladdin. Unless either noted, all of the solvents were used without further purification, and all solvents were either HPLC or spectroscopic grade in the optical spectroscopic studies. Silica gels (300-400 mesh) for column chromatography were purchased from Tansuo.

^{1}H NMR and ^{13}C NMR spectroscopy were measured on a Bruker AM400 NMR spectrometer. Chemical shifts of NMR spectra performed in ppm and we take tetramethylsilane (TMS, 0.00 ppm) as internals standard. High resolution mass spectrometry (HRMS) was recorded on a SHIMADZU LCMS-IT-TOF mass spectrometer. The X-ray intensity data were measured on a Bruker D8 VENTURE PHOTON III system equipped with a Incoatec Ius 3.0. Fluorescence emission spectra were obtained using Hitachi F-7000 spectrometer at 298 K. UV-Vis absorption spectra were recorded on a Hitachi UV-1900 UV-Visible Spectrophotometer. The absolute fluorescence quantum yields were collected on a Horiba Fluorolog-3 fluorescence spectrometer with a calibrated integrating sphere system. The fluorescence lifetime was measured using a Hamamatsu Compact Fluorescence Lifetime Spectrometer C11367. The viscosity of water/ glycerol or water/ glycerol mixtures were measured using an advanced Brook field Rheo3000 R/S plus Rheometer. The temperature was kept at (20 ± 0.1) °C with a bath circulator. Confocal lasing scanning microscopic (CLSM) images were obtained from LSM 780 (Zeiss). Fluorescence lifetime imaging microscopy(FLIM) images were collected on Nikon A1R MP+ laser scanning confocal microscope. Fluorescence quantum yield (Φ) was recorded on Fluorolog-3.

1.2 Reaction procedures

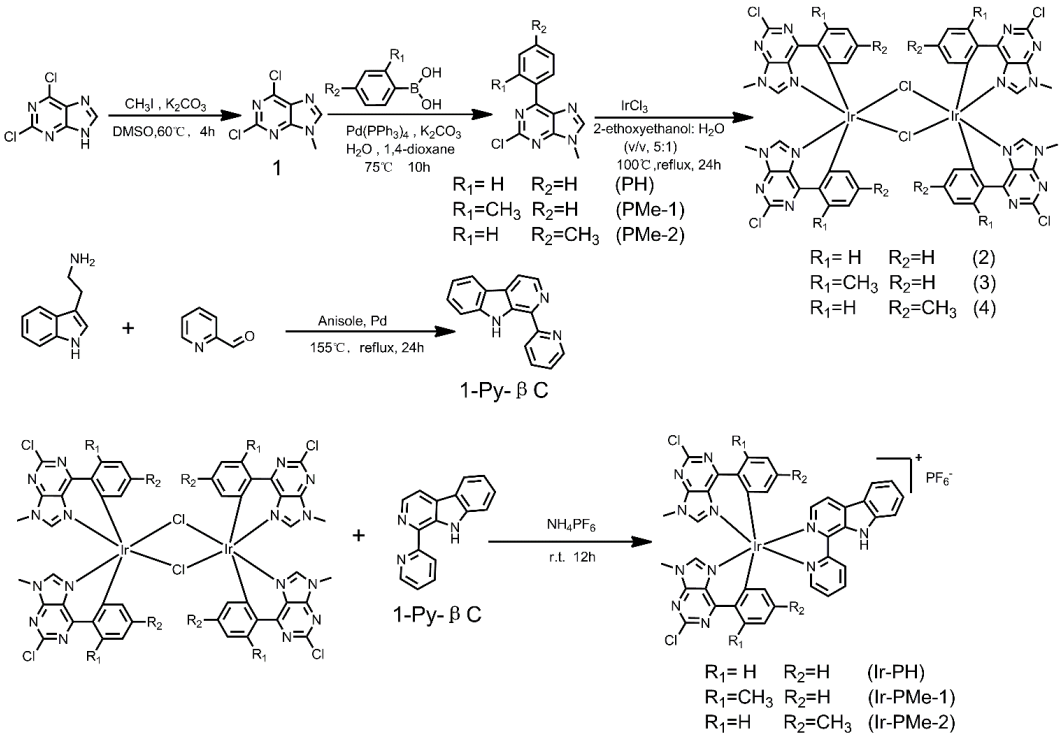

Scheme S1. The synthetic route of **Ir-PH, Ir-PMe-1** and **Ir-PMe-2**

Compound 1 was synthesized according to the literature method.[S1] **Compound 1** changed 1-bromopropane to methyl iodide.

Compound PH was produced according to the literature method. Compound 1 (1016 mg, 5 mmol), phenylboronic acid (670.6 mg, 5.5 mmol), $Pd(PPh_3)_4$ (288.8 mg,0.25 mmol) and K_2CO_3 (1104.0 mg,8 mmol) in 50 mL 1,4-dioxane and 10 mL water was refluxed for 8 hours under N_2, After the reaction was completed based on the TLC, poured the reaction mixture into water and extracted with DCM. The organic layer was washed with brine, water and dried over anhydrous Na_2SO_4. The crude product was purified by column chromatography on 200-300 mesh silica gel. Elution with DCM gave **PH** as a white solid in 82% yield. 1H NMR (400 MHz, CDCl3): δ (TMS, ppm) 8.80 – 8.76 (m, 2H), 8.08 (s, 1H), 7.56 (d, *J* = 1.7 Hz, 1H), 7.55 (d, *J* = 2.6 Hz, 2H), 3.91 (s, 3H).

Compound PMe-1 was produced using the same procedure as **compound PH** by changing the phenylboronic acid as 2-methylphenylboronic acid. **PMe-1** is white solid with 85% yield. ^{1}H NMR (400 MHz, $CDCl_3$): δ (TMS, ppm) 8.05 (s, 1H), 7.73 (d, *J* = 7.2 Hz, 1H), 7.42 – 7.37 (m, 1H), 7.34 (d, *J* = 6.4 Hz, 2H), 3.93 (s, 3H), 2.46 (s, 3H).

Compound PMe-2 was produced using the same procedure as **compound PH** by changing the phenylboronic acid as 4-methylphenylboronic acid. **PMe-2** is white solid with 78% yield. ^{1}H NMR (400 MHz, $CDCl_3$) δ 8.68 (d, J = 8.3 Hz, 2H), 8.03 (s, 1H), 7.33 (d, J = 8.0 Hz, 2H), 3.88 (s, 3H), 2.43 (s, 3H).

Compound 2(3/4) was synthesized according to the literature method.[S2] Yield 90% (78%/83%).

Complex Ir-PH The Ir(III) dimer $[(C\text{^}N)_2IrCl]_2$ **compound 2** (143.0 mg, 0.1 mmol), 1-Py-βC as the N^N ligand (49.6 mg, 0.2 mmol), were added in CH_2Cl_2 and MeOH (v/v = 1:1, 30 mL). The mixture was stirring for 10 h. After the reaction was completed, and NH_4PF_6 (163.0 mg,1 mmol) was added and kept stirring at r.t. for 2 h. Then, removal of the solvent and purification of the crude product by silica column chromatography. Then a bright yellow powder was obtained, 60.2 mg. Yield 28%。^{1}H NMR (400 MHz, DMSO-*d*$_6$) δ 12.28 (s, 1H), 8.85 (d, *J* = 8.2 Hz, 1H), 8.73 (dt, *J* = 7.9, 1.4 Hz, 2H), 8.38 (d, *J* = 5.7 Hz, 1H), 8.32 – 8.23 (m, 3H), 8.03 (d, *J* = 5.7 Hz, 1H), 7.89 (s, 1H), 7.78 (d, *J* = 8.3 Hz, 1H), 7.73 (s, 1H), 7.71 – 7.61 (m, 2H), 7.37 (td, *J* = 7.4, 7.0, 1.0 Hz, 1H), 7.09 (m, 2H), 6.75 – 6.70 (m, 2H), 6.35 (dd, *J* = 8.1, 2.8 Hz, 2H), 3.57 (d, *J* = 2.1 Hz, 6H). ^{13}C NMR (101 MHz, DMSO-*d*$_6$) δ 158.7, 158.6, 156.2, 155.2, 155.1, 152.7, 152.6, 150.8, 147.0, 146.6, 145.9, 142.9, 140.7, 140.5, 140.3, 139.1, 135.2, 133.8, 131.2, 131.0, 130.6, 130.4, 127.9, 127.8, 127.7, 126.5, 123.3, 122.6, 121.8, 120.8, 120.7, 120.2, 119.6, 113.1, 31.4. HRMS (ESI): m/z calcd for $[M\text{-}PF_6]^+$: 924.1457; Found: 924.1454.

Complex Ir-PMe-1 The Ir(III) dimer $[(C\text{^}N)_2IrCl]_2$ **compound 3** (148.6.0 mg, 0.1 mmol), 1-Py-βC as the N^N ligand (49.6 mg, 0.2 mmol), were added in CH_2Cl_2 and MeOH (v/v = 1:1, 30 mL). The mixture was stirring for 10 h. After the reaction was completed, and NH_4PF_6 (143.0 mg, 0.1 mmol) was added and kept stirring at r.t. for 2 h. Then, removal of the solvent and purification of the crude product by silica column chromatography. Then a yellow powder was obtained, 52.8 mg. Yield 24%. ^{1}H NMR (400 MHz, DMSO-*d*$_6$) δ 12.21 (s, 1H), 8.78 (d, J = 8.3 Hz, 1H), 8.45 – 8.39 (m, 2H), 8.30 – 8.24 (m, 2H), 8.19 (d, J = 5.7 Hz, 1H), 7.83 (s, 1H), 7.76 (d, J = 8.3 Hz, 1H), 7.70 – 7.64 (m, 3H), 7.40 (m, 1H), 6.91-6.86 (m, 2H), 6.53 (td, J = 7.6, 2.6 Hz, 2H), 6.35 – 6.30 (m, 2H), 3.54 (s, 6H), 2.97 (s, 6H). ^{13}C NMR (101 MHz, DMSO-*d*$_6$) δ 160.4, 160.3, 156.2, 153.4, 153.3, 152.2, 150.8, 149.6, 149.0, 145.7, 142.9, 141.3, 141.1, 140.5, 140.4, 140.4, 140.2, 139.2, 135.1, 133.7, 131.2, 129.8, 129.7, 129.4, 128.8, 127.5, 126.4, 122.7, 122.6, 122.4, 121.8, 120.2, 119.5, 113.1, 31.3, 28.3, 28.2. HRMS (ESI): m/z calcd for $[M\text{-}PF_6]^+$: 952.1770; Found:.952.1772.

Complex Ir-PMe-2 The Ir(III) dimer $[(C\text{^}N)_2IrCl]_2$ **compound 4** (148.6 mg, 0.1 mmol), 1-Py-βC as

the N^N ligand (49.6 mg, 0.2 mmol), were added in CH_2Cl_2 and MeOH (v/v = 1:1, 30 mL). The mixture was stirring for 10 h. After the reaction was completed, and NH_4PF_6 (143.0 mg, 0.1 mmol) was added and kept stirring at r.t. for 2 h. Then, removal of the solvent and purification of the crude product by silica column chromatography. Then a yellow powder was obtained, 87.8 mg. Yield 40%. ^{1}H NMR (400 MHz, CD_2Cl_2) δ 10.14 (s, 1H), 8.83 (dd, J = 8.2, 3.9 Hz, 2H), 8.74 (d, J = 7.9 Hz, 1H), 8.45 – 8.39 (m, 1H), 8.21 (d, J = 5.7 Hz, 2H), 8.12 (d, J = 8.0 Hz, 1H), 8.00 (d, J = 5.6 Hz, 1H), 7.84 (d, J = 8.3 Hz, 1H), 7.64 (s, 1H), 7.43 – 7.34 (m, 2H), 7.03 (dt, J = 6.6, 1.5 Hz, 3H), 6.94 (s, 1H), 6.12 (dt, J = 15.2, 1.2 Hz, 2H), 3.67 (d, J = 2.1 Hz, 6H), 1.93 (s, 6H). ^{13}C NMR (101 MHz, CD_2Cl_2) δ 159.63, 150.36, 144.83, 143.25, 142.90, 141.70, 140.72, 140.55, 140.37, 139.32, 128.64, 126.91, 126.82, 125.07, 124.96, 122.09, 121.72, 119.83, 118.74, 113.31, 31.10, 21.64, 21.59. HRMS (ESI): m/z calcd for $[M\text{-}PF_6]^+$: 952.1770; Found:.952.1772.

1.3 Cell culture

A549, 7702 cells were cultured in RPMI Medium 1640 basic (1X) containing 10 % fetal bovine serum and 1 % Antibiotic–antimycotic at 37 ℃ in a 5 % CO_2/95 % air incubator.

HepG 2 cells were cultured in Dulbecco's modified Eagle medium (DMEM) containing 10% fetal bovine serum and 1% Antibiotic– antimycotic at 37℃ in a 5% CO_2/95% air incubator.

1.4 Toxicity Studies.

Toxicities of **Ir-PH**, **Ir-PMe-1** and **Ir-PMe-2** toward A549 cells was determined by MTS (3-(4,5-dimethylthiazol-2-yl)-5-(3-carboxymethoxyphenyl)-2-(4-sulfophenyl)-2H-tetrazolium) reduction assay following literature procedures. About 10000 cells per well were seeded in 96-well plates and cultured overnight for 70-80% cell confluence. The medium was replaced with 100 μL of fresh medium with different concentration (20 μM, 10 μM, 5 μM, 2.5 μM, 1.25 μM, blank) of **Ir-PH**, **Ir-PMe-1** or **Ir-PMe-2**. 24 hours later, 100 μL of 20% MTS solution in PBS was replaced with the old medium in each well for another approximately 30 min at 37 ℃ incubation. Then the absorption of each well was tested at wavelength of 490 nm. The metabolic activity of the **Ir-PH**, **Ir-PMe-1** or **Ir-PMe-2** treated cells was expressed as compared with untreated cell controls taken as 100% metabolic activity.

1.5 Cell imaging

A549, 7702, HepG 2 were seeded in 35 mm confocal dish (Φ = 15 mm) and grown overnight. The cells were stained with **Ir-PH** (2 μM), **Ir-PMe-1** (2 μM) or **Ir-PMe-2** (2 μM) at 30 min, then washed with 1 mL PBS three times. The cells were imaged under CLSM using proper excitation and emission of **Ir-PH**, **Ir-PMe-1** and **Ir-PMe-2**: λ_{ex}=405 nm, λ_{em}=500-600 nm

1.6 Co-localization imaging

A549, 7702, HepG 2 were seeded in 35 mm confocal dish (Φ = 20 mm) and grown overnight. The cells were treated by **Ir-PH** (2 μM, λ_{ex}=405 nm), **Ir-PMe-1** (2 μM, λ_{ex}=405 nm) and **Ir-PMe-2** (2 μM, λ_{ex}=405 nm) with commercial dyes, Endoplasmic Reticulum Tracker Red (ERTR, λ_{ex}=543 nm), Mito-Tracker deep Red (MTDR, λ_{ex}=633 nm), Lyso-Tracker deep Red (LTDR, λ_{ex}=633 nm) incubation for 30 min, respectively. Then confocal images were recorded by LSM 780 (Zeiss) after washed them with PBS three times.

1.7 Fluorescence visualization of viscosity changes under ER stress

About 10000 A549 cells per well were seeded in 96-well plates and cultured overnight. A549 cells were incubated with **Ir-PH** for 30 min and different concentrations (blank, 10 μg/mL, 20 μg/mL, 50 μg/mL, 70 μg/mL) of tunicamycin (Tm) for 30 min and recorded by CLSM and microplate reader (SPARK).

1.8 Fluorescence Lifetime Imaging Microscopy (FLIM)

A549 were seeded in 35 mm confocal dish (Φ = 20 mm) and grown overnight. A549 cells were incubated with 5 μM **Ir-PH** for 30 min and different concentrations Tm (blank, 10 μg/mL, 20 μg/mL, 30 μg/mL, 40 μg/mL, 50 μg/mL) for 20 min. Then washed with PBS three times and were collected on Nikon A1R MP+ laser scanning confocal microscope.

2. Single-crystal structure determination

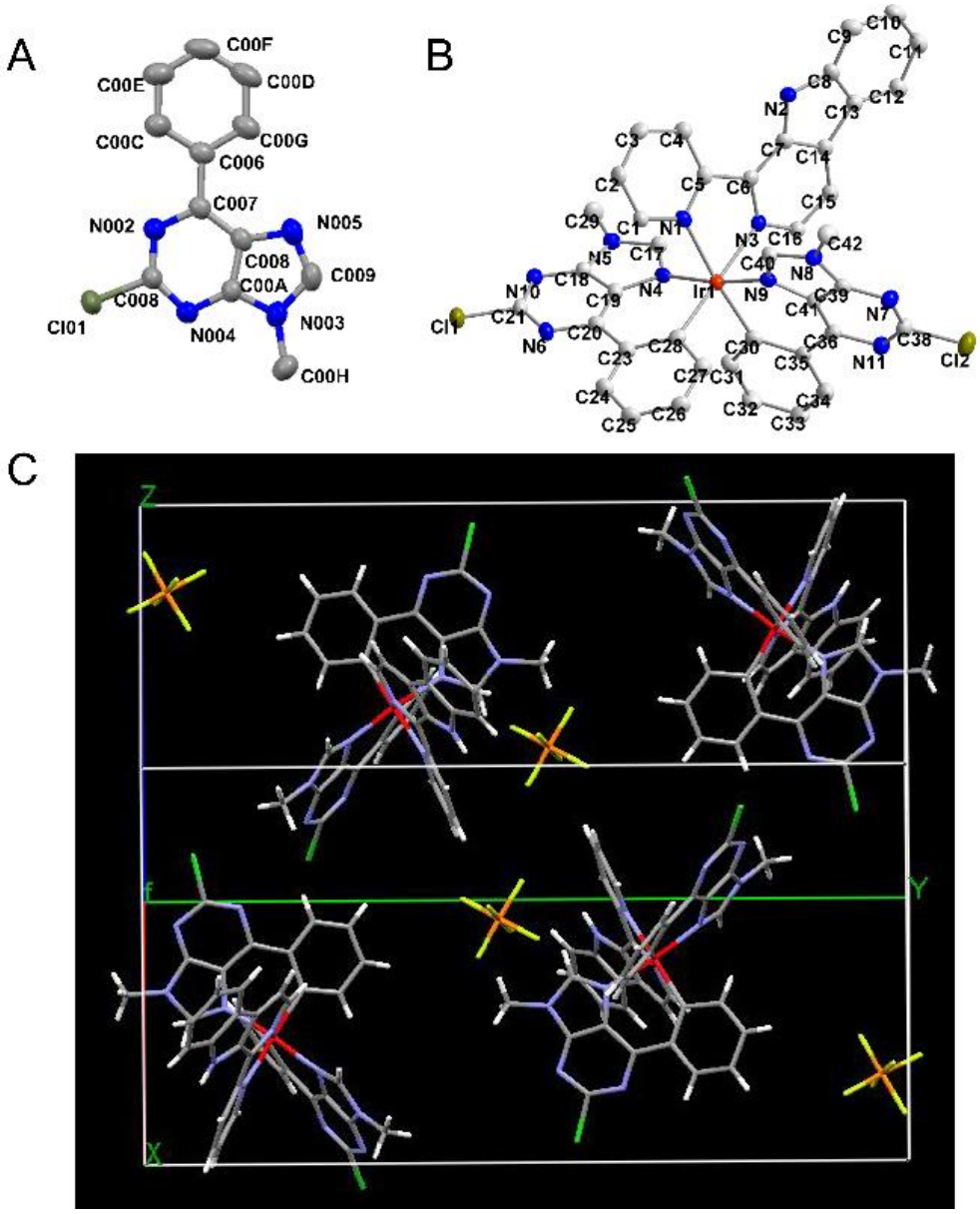

Figure S1. (A) the ORTEP representation of Compound **PH**. (B) the ORTEP representation of Compound **Ir-PH**. (C) Unit cell of **Ir-PH**. The solvent have been omitted for clarity. Carbon, hydrogen, nitrogen and iridium atoms are shown in grey, white, blue, and red, respectively

Table S1. Crystallographic data of **PH** and **Ir-PH**

Compounds	**PH**	**Ir-PH**•$4CH_2Cl_2$
Formula	$C_{12}H_9ClN_4$	$C_{44}H_{35}Cl_{10}F_6IrN_{11}P$
Molecular weight	244.68	1409.50
Temperature/K	297.5 (2)	190(2)
Wavelength/ Å	1.54184	1.54184
Crystal size/mm^3	0.6 × 0.4 × 0.2	0.1 × 0.1 × 0.1
Crystal system	monoclinic	monoclinic
Space group	$P2_1/n$	$P2_1/n$
a/Å	6.9944(5)	12.614(2)
b/Å	11.3189(5)	27.595(4)
c/Å	14.3507(7)	15.860(5)
α/°	90	90
β/°	98.083(5)	113.041
γ/°	90	90
Volume/$Å^3$	1124.84(11)	5080.(2)
Z	4	4
Density (calculated)g/cm^3	1.445	1.843
Absorption coefficient/mm^{-1}	2.851	10.830
F(000)	504.0	2768
Goodness-of-fit on F^2	1.085	1.040
$R_1[I > 2\sigma(I)]$	0.0716	0.0348
WR_2	0.1887	0.0884

Table S2. Selected bond lengths and bond angles of **PH** and **Ir-PH**

Compounds	**PH**		**Ir-PH**•$4CH_2Cl_2$	
Bond lengths(Å)	N002-C007	1.350(3)	Ir-PH-N9	2.023(4)
	N002-C00B	1.310(3)	Ir-PH-N4	2.035(4)
	N005-C008	1.383(3)	Ir-PH-C30	2.061(4)
	N005-C009	1.307(4)	Ir-PH-C28	2.061(4)

	C006-C00G	1.390(4)	Ir-PH-N1	2.122(4)
	C00D-C00G	1.393(4)	Ir-PH-N3	2.144(4)
Bond angles (º)	C009-N005-C008 104.0(2)		N4-Ir-PH-C28	91.07(15)
	C00B-N002-C007 118.1(2)		N4-Ir-PH-N1	84.18(13)
	C006-C00G-C00D 119.9(3)		C28-Ir-PH-N1	100.15(15)
			N4-Ir-PH-N3	91.93(13)
			C28-Ir-PH-N3	175.89(15)
			N1-Ir-PH-N3	77.37(13)
Torsion angles(°)	C00G-C006-C007-C008 5.70		N1-C5-C6-N3	15.1(5)
	C00C-C006-C007-N002 5.24		C4-C5-C6-C7	18.6(7)
			N6-C20-C23-C24	11.0(6)
			C19-C20-C23-C28	10.3(7)

3. Molar Extinction Coefficient of Ir-PH、Ir-PMe-1 and Ir-PMe-2

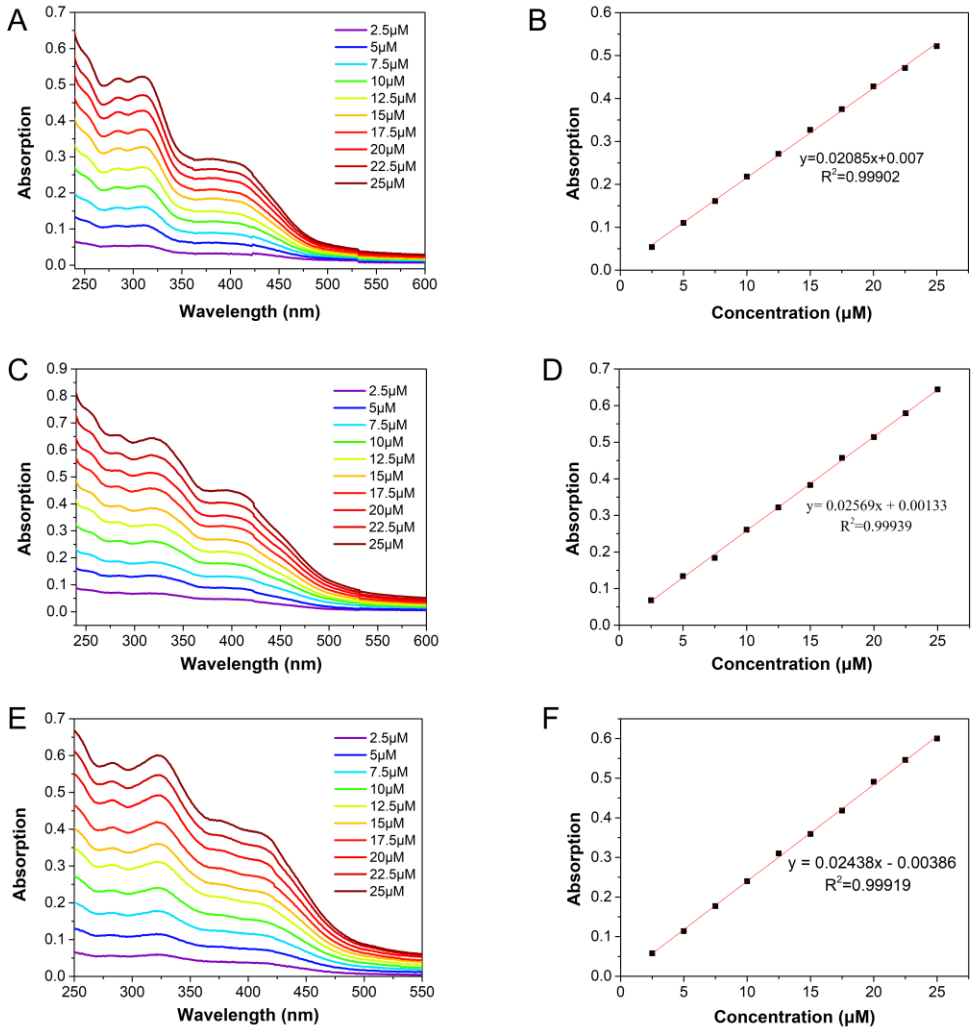

Figure S2. UV/Vis spectra of A) **Ir-PH** C) **Ir-PMe-1** E) **Ir-PMe-2** at different concentrations (2.5, 5,7.5,10, 12.5, 15, 17.5, 20, 22.5, 25 μM); Absorption-concentration curve of B) **Ir-PH** D) **Ir-PMe-1** F) **Ir-PMe-2.**

4. Metal ions interference experiment

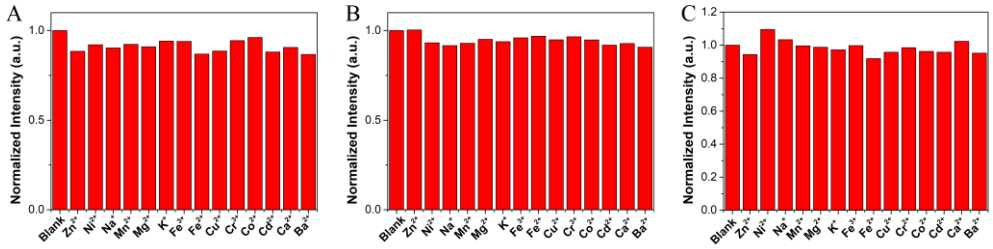

Figure S3. (A) Fluorescence normalized intensity of **Ir-PH** (10 μM) with metal ions (50 μM) at 550 nm; (B) Fluorescence normalized intensity of **Ir-PMe-1** (10 μM) with metal ions(50 μM) at 570 nm;

(C) Fluorescence normalized intensity of **Ir-PMe-2** (10 μM) with metal ions(50 μM) at 550 nm.

5. Polarity-response

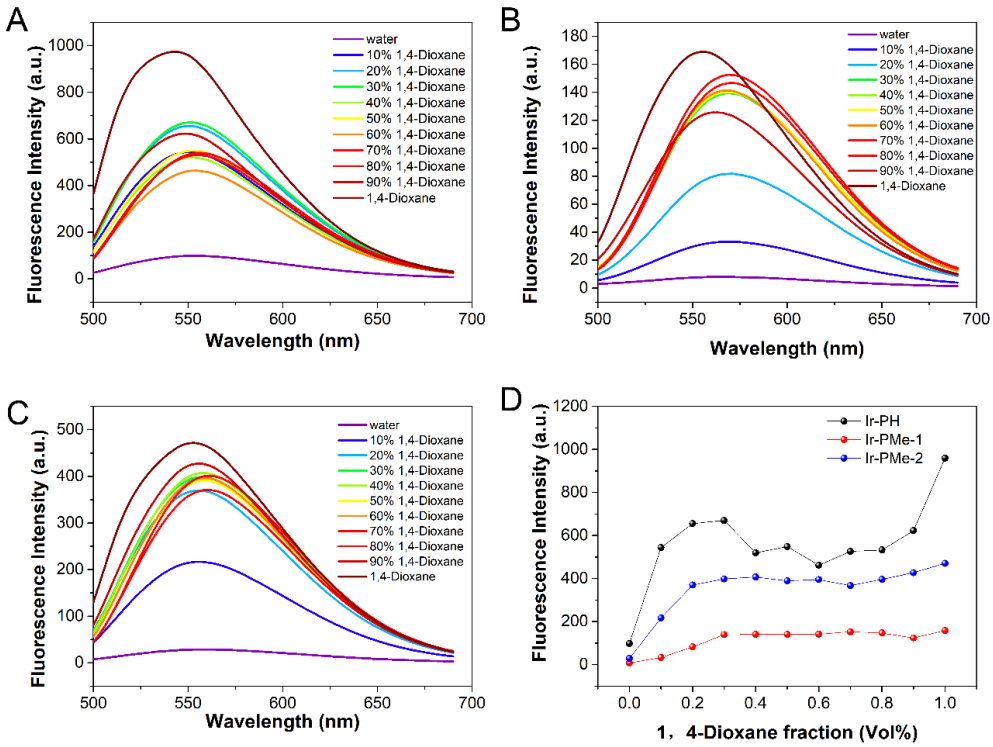

Figure S4. Fluorescence spectra of A) **Ir-PH** (10 μM) B) **Ir-PMe-1** (10 μM) C) **Ir-PMe-2** (10 μM) in variety fraction of water-1,4-dioxane system; D) Fluorescence emission intensity-polarity curves.

6. Fluorescence spectra and fluorescent lifetime of Ir-PMe-1 and Ir-PMe-2 in Glycerol/Water mixtures

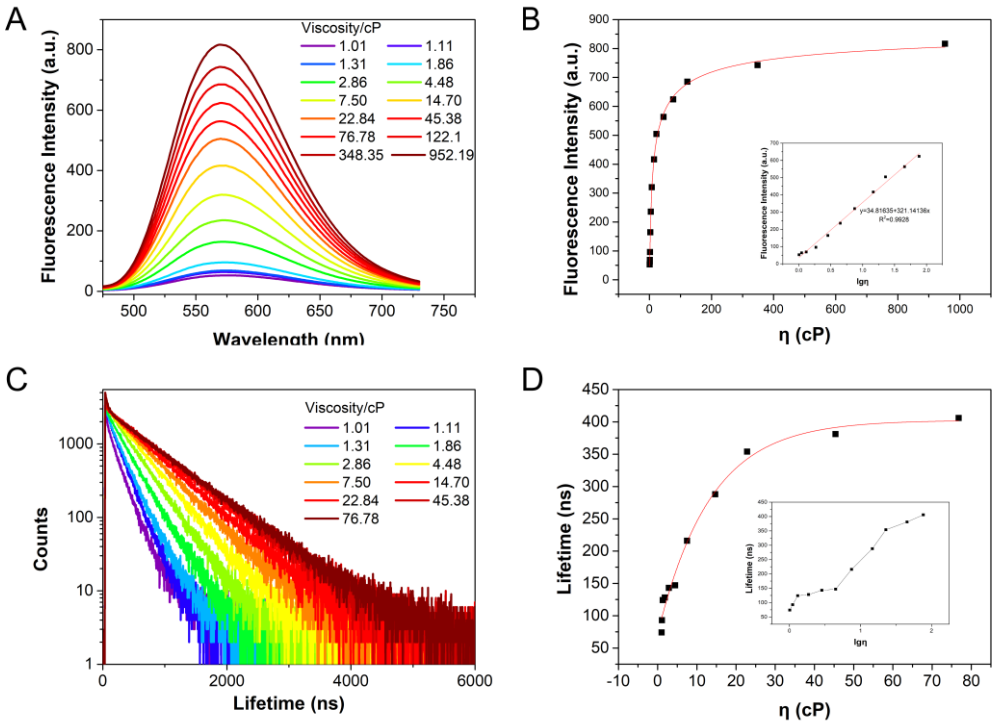

Figure S5. (A)Fluorescence emission intensity and (C) lifetime of **Ir-PMe-1** (10 μM) in mixtures of water and glycerol at different viscosity (1.01, 1.11, 1.31, 1.86, 2.86, 4.48, 7.50, 14.70, 22.84, 45.38, 76.78 cP); (B) Fluorescence emission intensity-viscosity curves; (D) Fluorescence lifetime-viscosity curves.

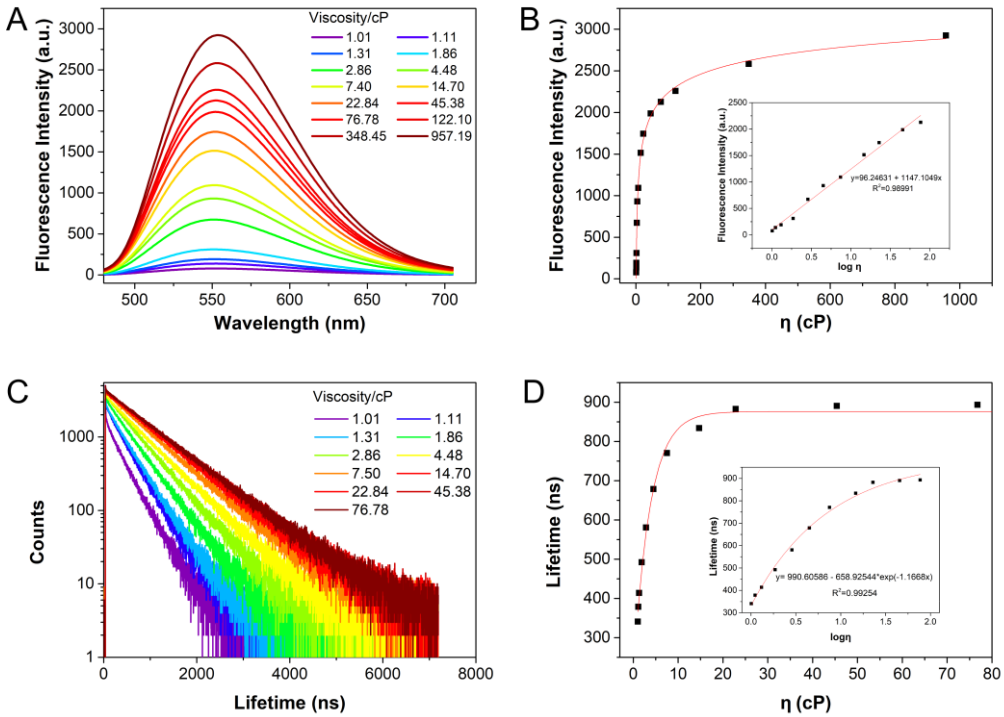

Figure S6. (A)Fluorescence emission intensity and (C) lifetime of **Ir-PMe-2** (10 μM) in mixtures of water and glycerol at different viscosity (1.01, 1.11, 1.31, 1.86, 2.86, 4.48, 7.50, 14.70, 22.84, 45.38, 76.78 cP); (B) Fluorescence emission intensity-viscosity curves; (D) Fluorescence lifetime-viscosity curves.

Table S3. Photophysical data of **Ir-PH**, **Ir-PMe-1 and Ir-PMe-2**

Compounds	λ_{Abs}[a] (nm)	λ_{em}[b] (nm)	ε[a] (M^{-1} cm^{-2})	Φ[b]	Φ[c]	Φ[d]
Ir-PH	284, 310, 406	550	2.09×10^4	0.10	0.08	0.43
Ir-PMe-1	285, 320, 406	570	2.57×10^4	<0.01	<0.01	0.11
Ir-PMe-2	282,324, 412	552	2.44×10^4	<0.01	0.03	0.36

[a] ε is the molar extinction coefficient measured in PBS; [b] Luminescence quantum yield is measured in solid state; [c] Luminescence quantum yield is measured in H_2O; [d] Luminescence quantum yield is measured in Glycerol.

7. Cytotoxicity experiments

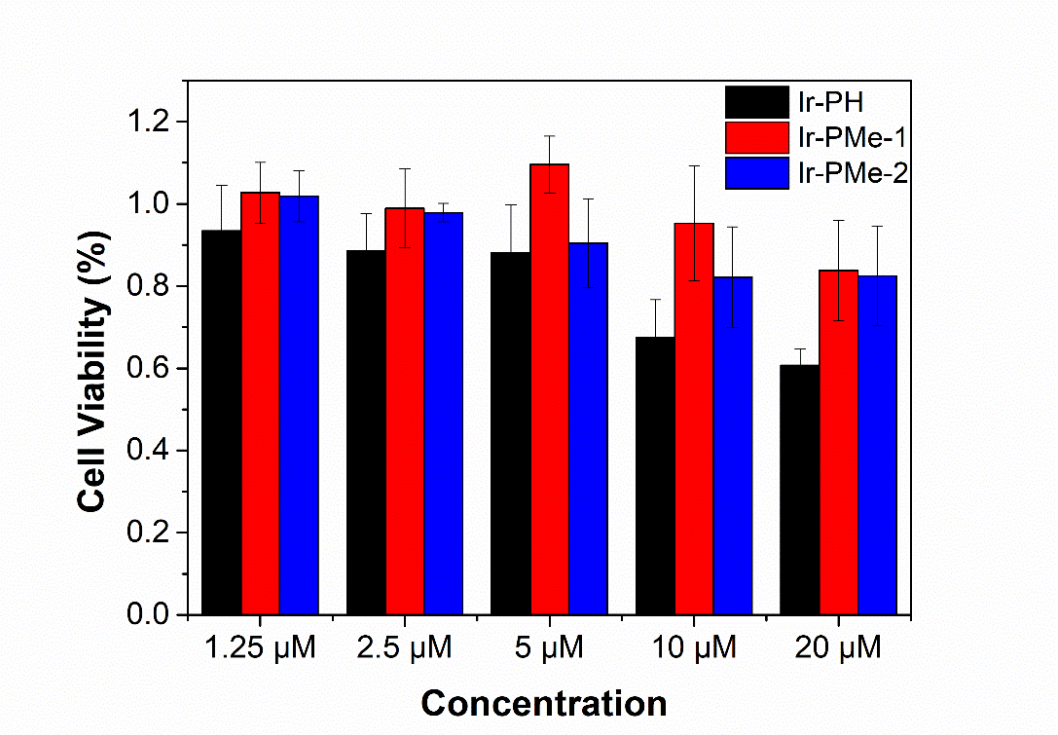

Figure S7. Cytotoxicity of **Ir-PH**, **Ir-PMe-1**, **Ir-PMe-2** at different concentrations (1.25, 2.5, 5, 10, 20 μM) in A549 cells.

8. Co-localization experiments of Ir-PH in different cells.

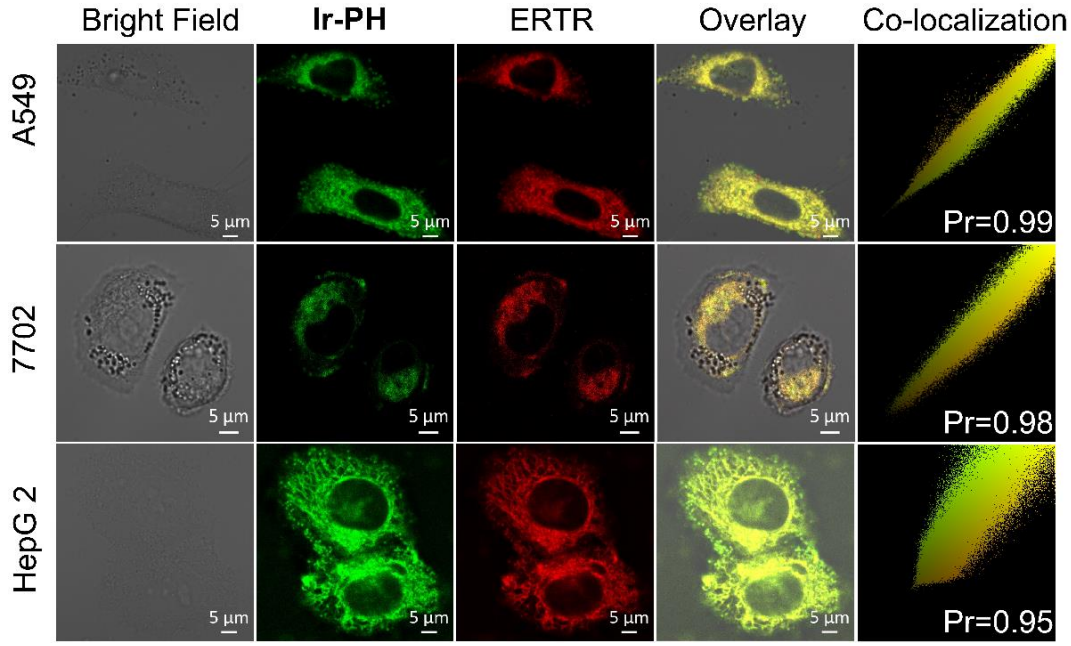

Figure S8. Cellular colocalization microscopy image of A549 cells, 7702 cells and HepG 2 cells incubated with **Ir-PH** (2 μM, λ_{ex}=405 nm, λ_{em}=500-600 nm) and ER-Tracker Red (ERTR) (500 nm,

λ_{ex}=543 nm, λ_{em}=600-650 nm).

9. Co-localization experiments of all complexes in subcellular organelles.

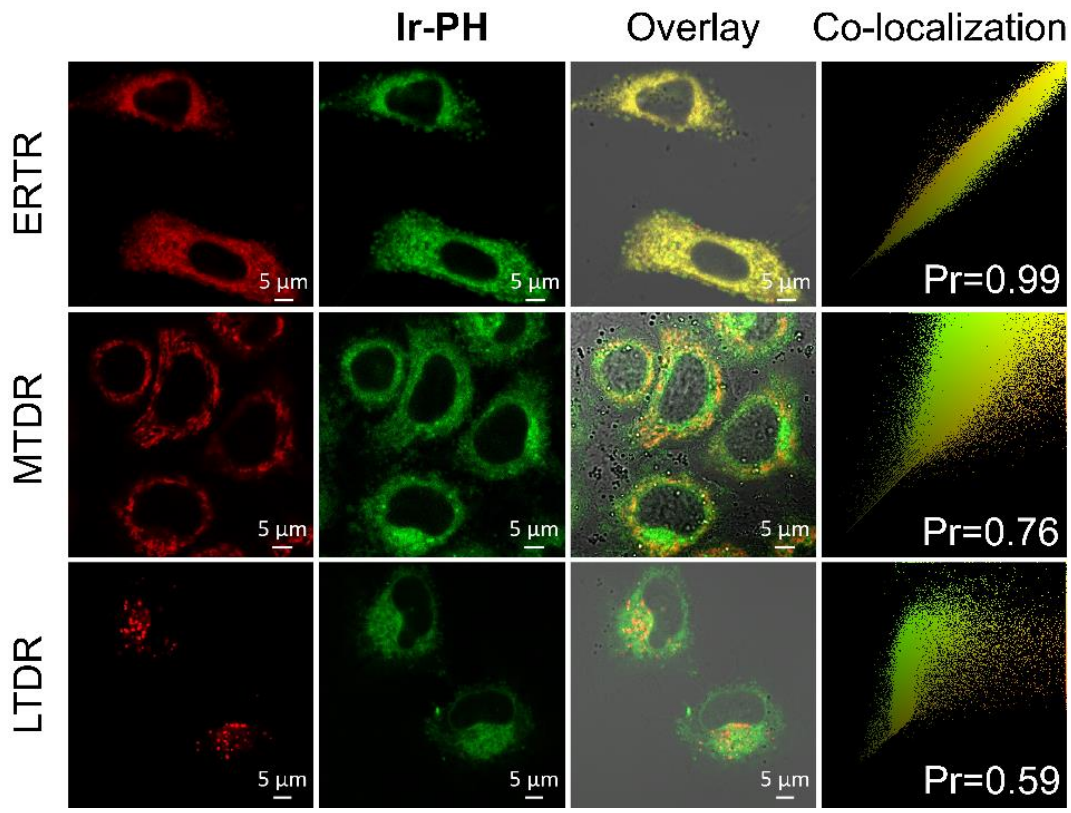

Figure S9. Confocal image of A549 cells incubated with **Ir-PH** (2 μM, λ_{ex}=405 nm, λ_{em}=500-600 nm) and ER-Tracker Red (ERTR) (500 nm, λ_{ex}=543 nm, λ_{em}=600-650 nm), Mito-Tracker deep Red (MTDR) (500 nM, λ_{ex}==633 nm, λ_{em}=650-700 nm), Lyso- Tracker deep Red (LTDR) (200 nM, λ_{ex}==633 nm, λ_{em}=650-700 nm).

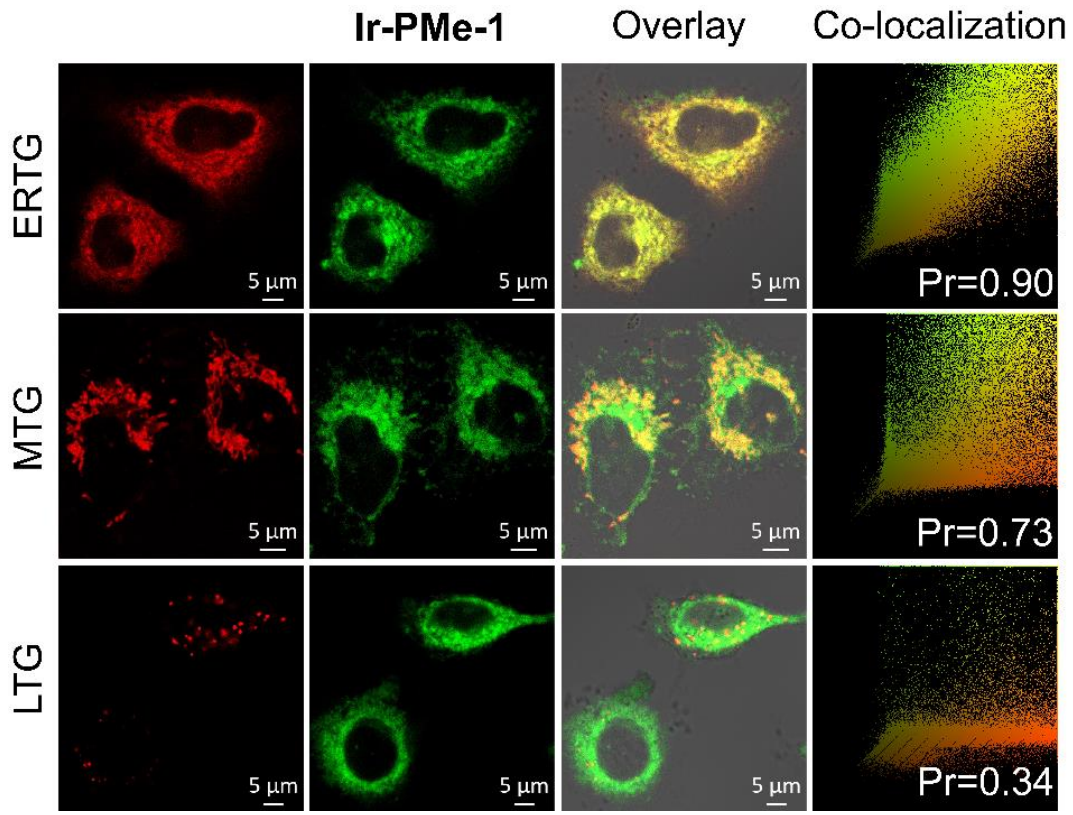

Figure S10. Confocal image of A549 cells incubated with **Ir-PMe-1** (2 μM, λ_{ex}=405 nm, λ_{em}=520-620 nm) and ER-Tracker Green (ERTG) (500 nm, λ_{ex}=488 nm, λ_{em}=500-520nm), Mito-Tracker Green (MTG) (500 nm, λ_{ex}=488 nm, λ_{em}=500-520 nm), Lyso- Tracker Green (LTG) (200 nm, λ_{ex}=488 nm, λ_{em}=500-520 nm).

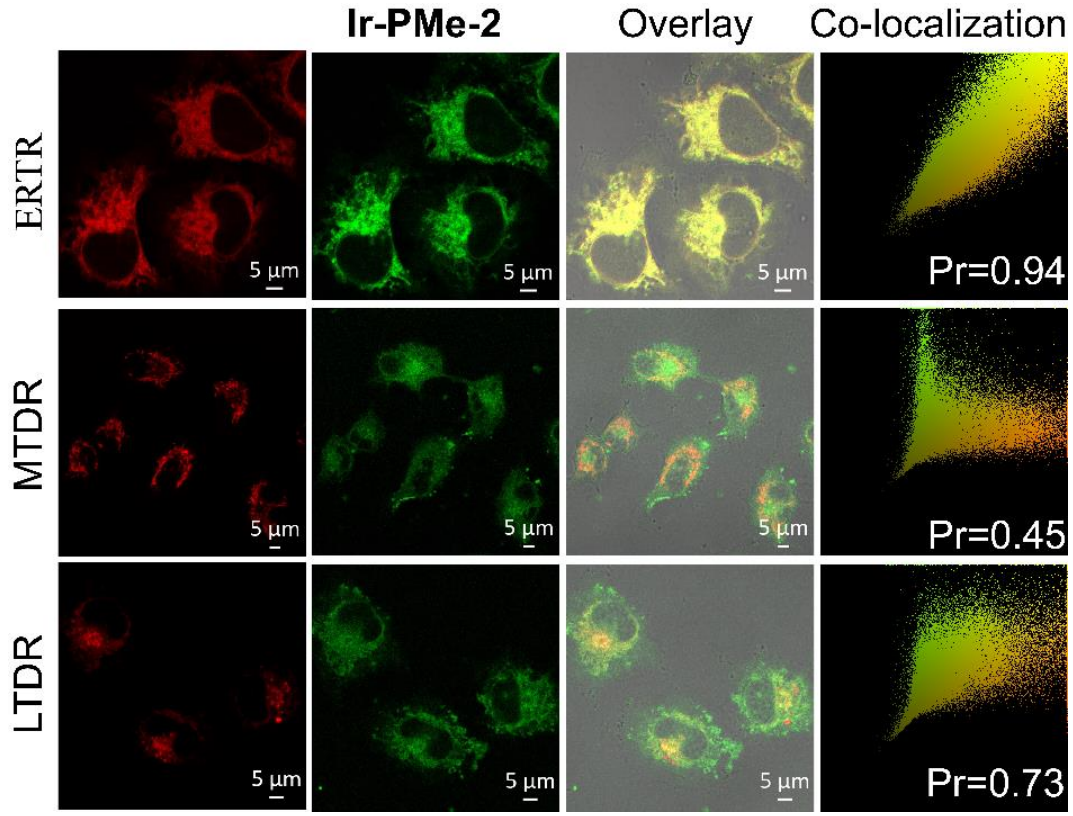

Figure S11. Confocal image of A549 cells incubated with **Ir-PMe-2** (2 μM, λ_{ex}=405 nm, λ_{em}=500-600 nm) and ER-Tracker Red (ERTR) (500 nm, λ_{ex}=543 nm, λ_{em}=600-650 nm), Mito-Tracker deep

Red (MTDR) (500 nM, λ_{ex}==633 nm, λ_{em}=650-700 nm), Lyso- Tracker deep Red (LTDR) (200 nM, λ_{ex}=633 nm, λ_{em}=650-700 nm).

10. CLSM of Ir-PH with Tm

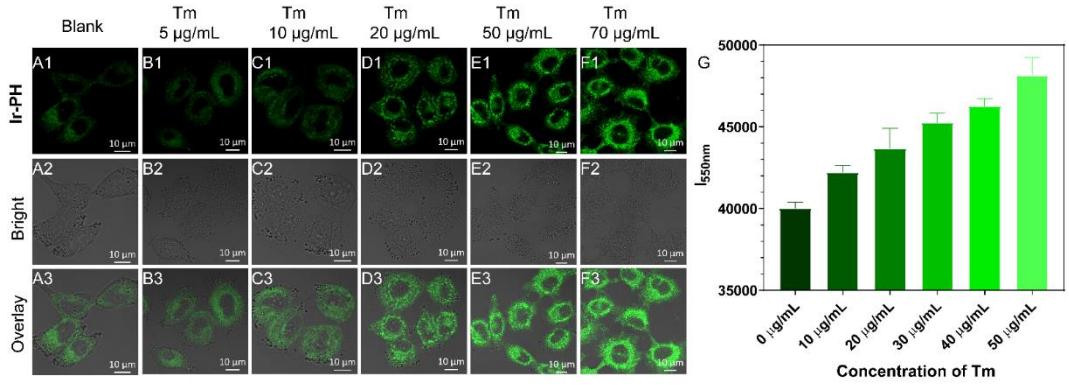

Figure S12. (A1-F3) Fluorescence images of **Ir-PH** (2 μM) in live A549 cells at 30 min and treated with Tm for 30 min at different concentrations (blank, 5 μg/mL, 10 μg/mL, 20 μg/mL, 50 μg/mL, 70 μg/mL), (G). The average intensity in A549 cells.

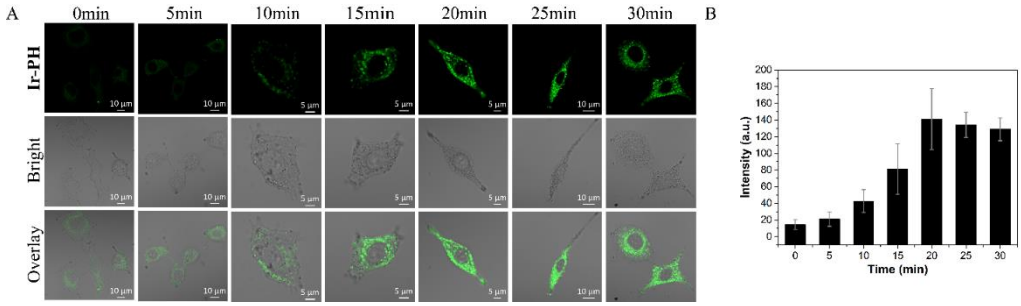

Figure S13. (A) CLSM of **Ir-PH** (2 μM) with Tm (50 μg/mL) at different time (0 min, 5 min, 10 min, 15 min, 20 min, 25 min, 30 min) in A549 cells. (B)The intensity of CLSM-time curves.

11. Photostability of the complexes

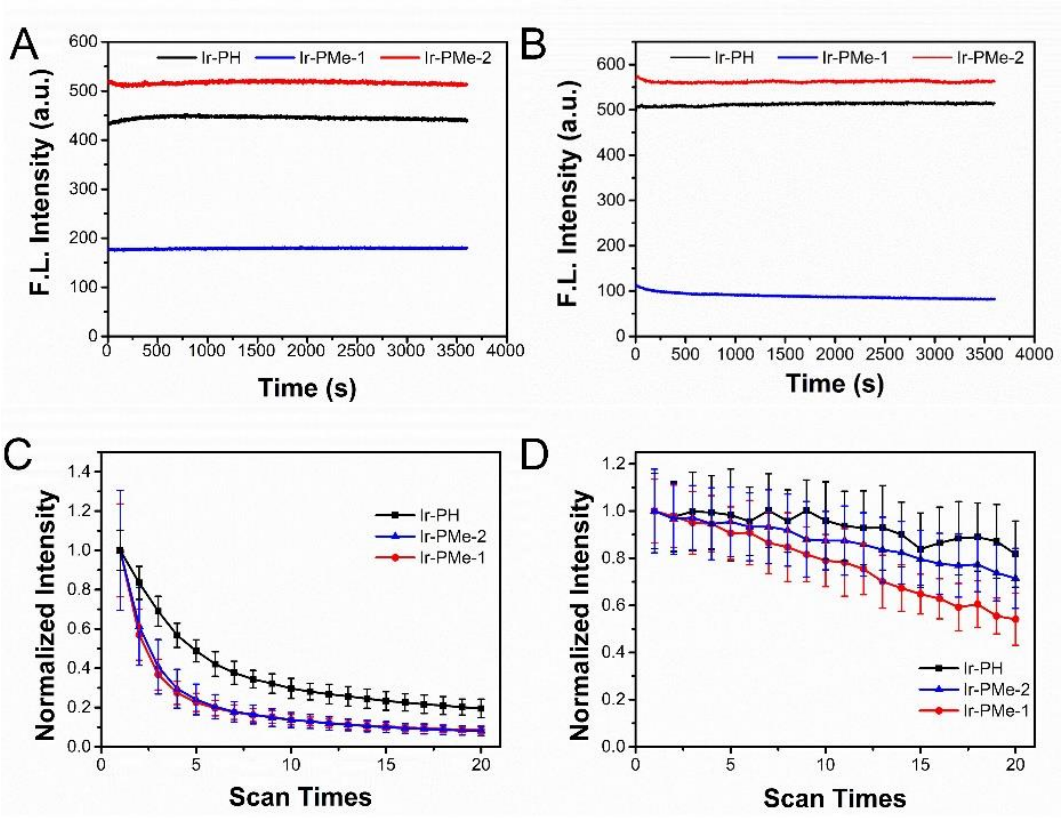

Figure S14. (A)The photostability of three complexes (10 μM) in N_2-saturated water solution; (B)The photostability of three complexes (10 μM) in air-saturated water solution; (C) The photostability of three complexes (2 μM) in A549, laser power: 100%. (D) The photostability of three complexes (2 μM) in A549, laser power: 2%.

12. NMR Data

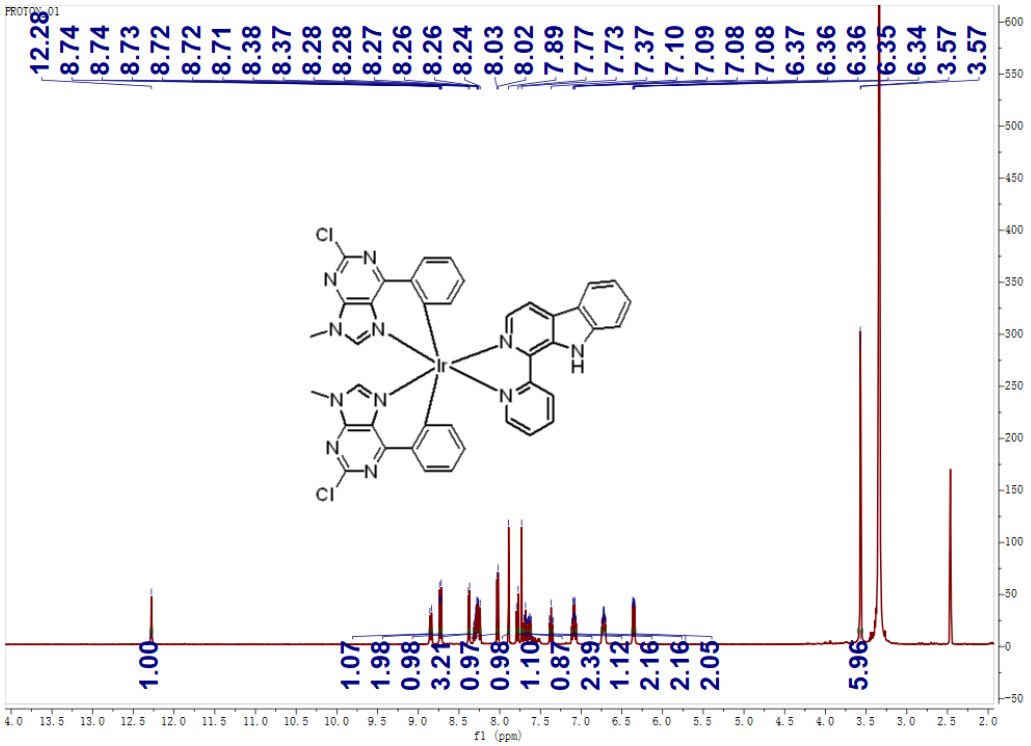

Figure S15. ^{1}H NMR spectrum of **Ir-PH** in DMSO-*d*$_6$

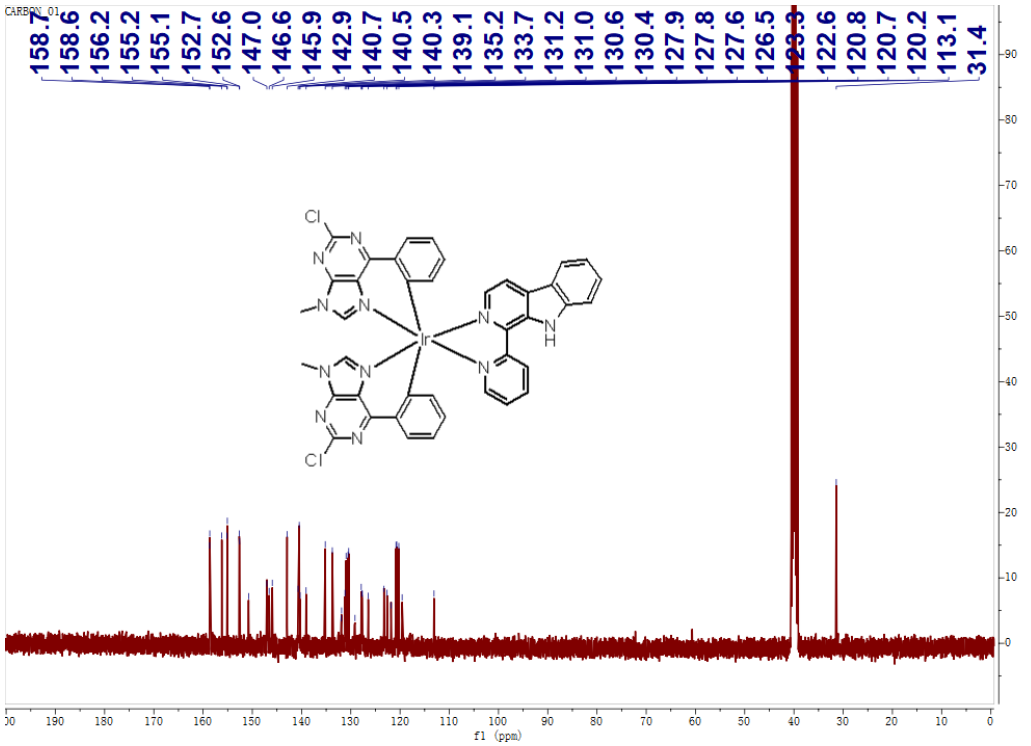

Figure S16. ^{13}C NMR spectrum of **Ir-PH** in DMSO-*d*$_6$

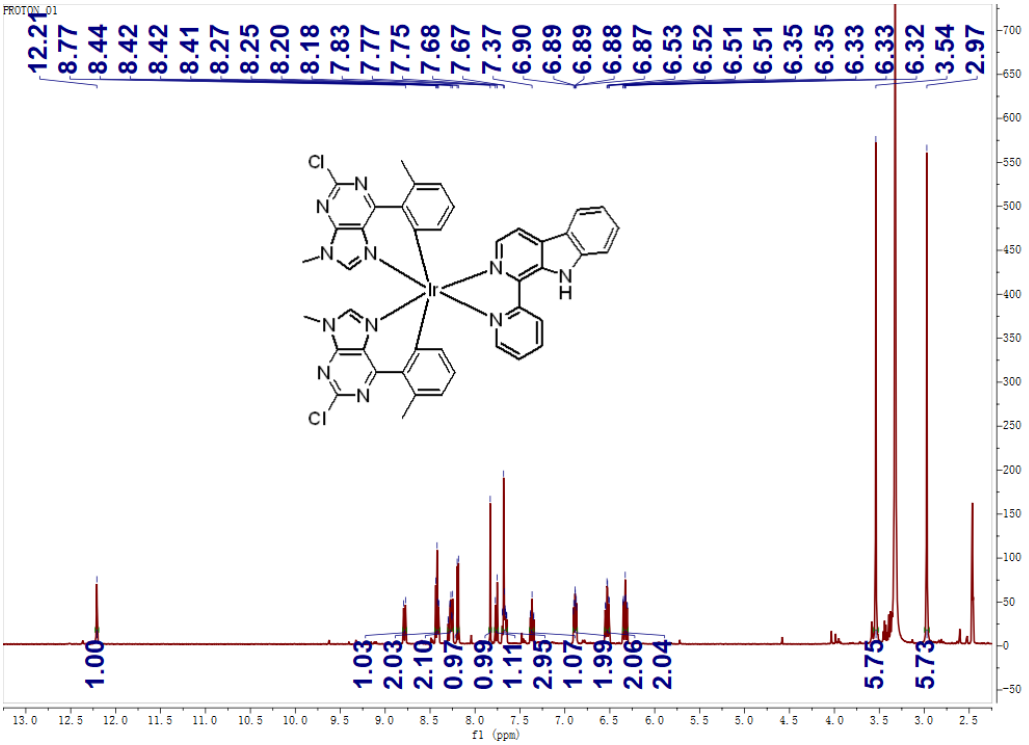

Figure S17. ^{1}H NMR spectrum of **Ir-PMe-1** in DMSO-*d*$_6$

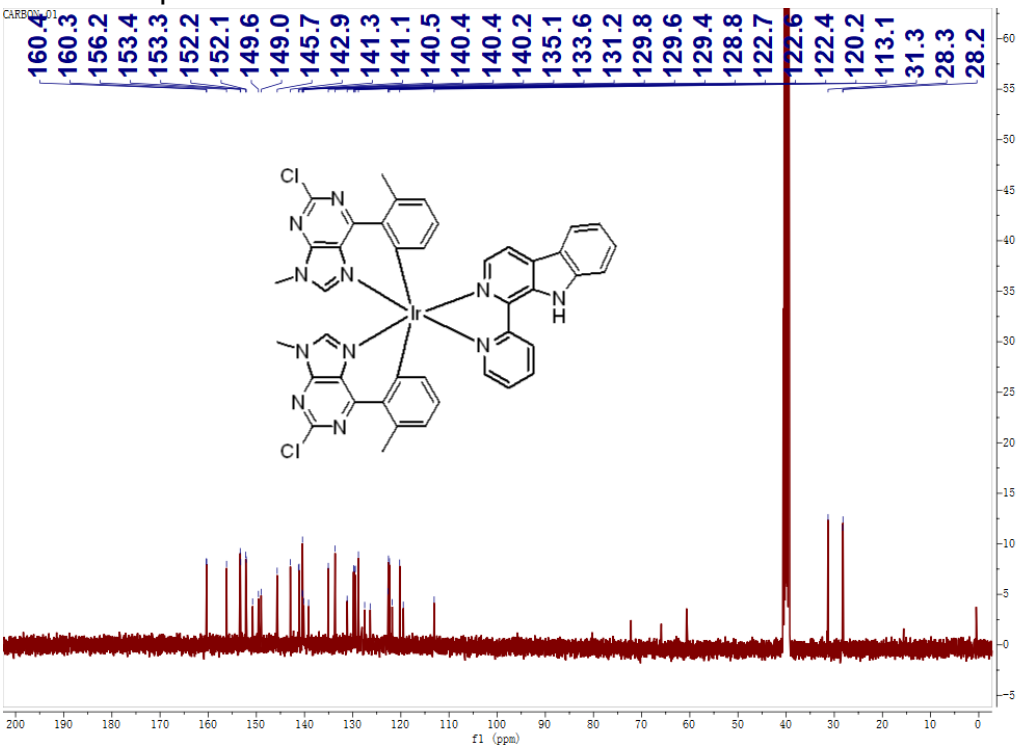

Figure S18. ^{13}C NMR spectrum of **Ir-PMe-1** in DMSO-*d*$_6$

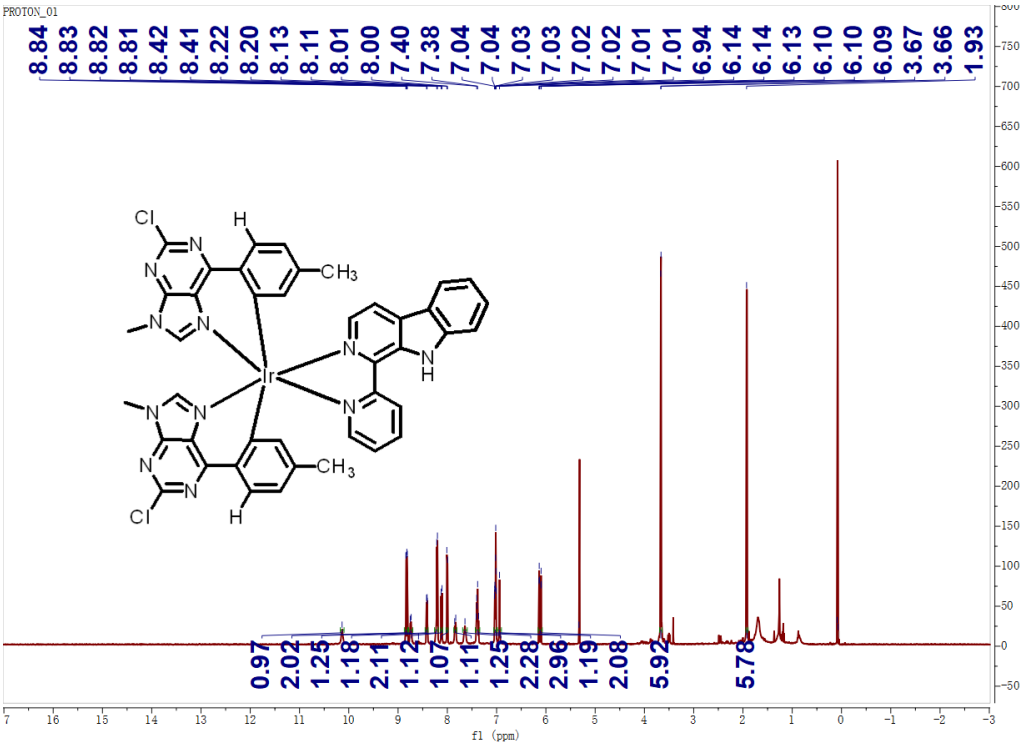

Figure S19. ^{1}H NMR spectrum of **Ir-PMe-2** in CD_2Cl_2

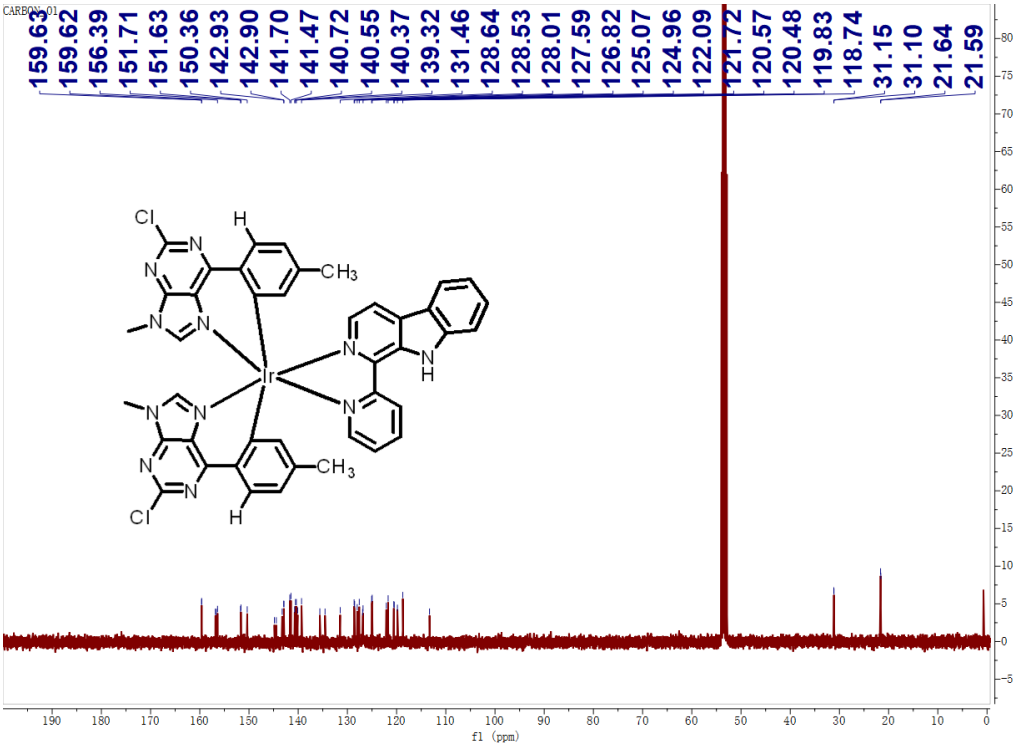

Figure S20. ^{13}C NMR spectrum of **Ir-PMe-2** in CD_2Cl_2

13. ESI-HRMS Data

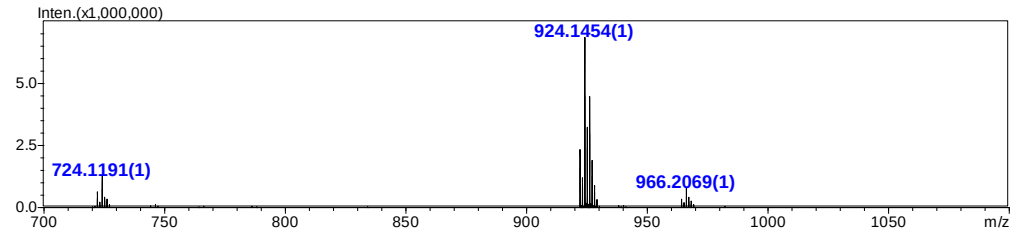

Figure S21. HRMS result of **Ir-PH.**

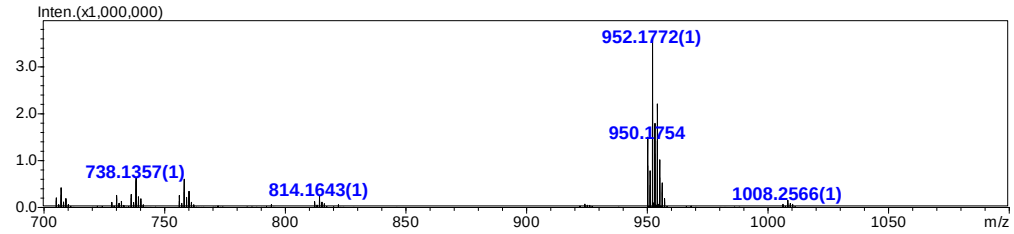

Figure S21. HRMS result of **Ir-PMe-1.**

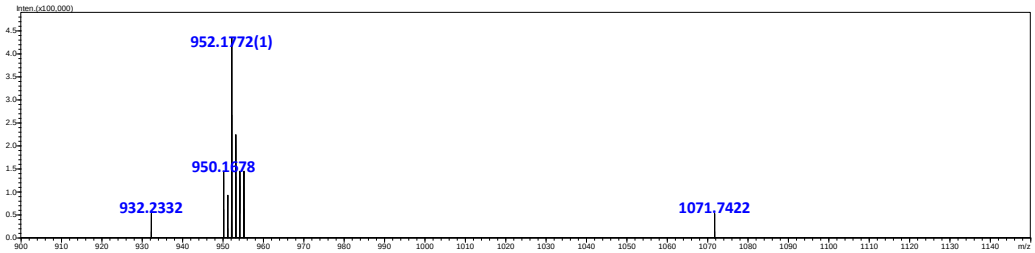

Figure S23. HRMS result of **Ir-PMe-2.**

References:

S1 L. Shi, K. Li, L.-L. Li, S.-Y. Chen, M.-Y. Li, Q. Zhou, N. Wang and X.-Q. Yu, *Chem. Sci.* 2018, **9**, 8969-8974.

S2 C.-H Yang, S.-W Li, Y. Chi, Y.-W. Cheng, Y.-S. Yeh, P.-T. Chou, G.-H. Lee, C.-H. Wang and C.-F. Shu, *Inorg. Chem.* 2005, **44**, 7770-7780.